

Locally Adaptive Smoothing for Functional Data

Tomoya Wakayama*

Graduate School of Economics, The University of Tokyo

and

Shonosuke Sugasawa

Center for Spatial Information Science, The University of Tokyo

July 27, 2021

Abstract

Despite increasing accessibility to function data, effective methods for flexibly estimating underlying trend structures are still scarce. We thereby develop locally adaptive smoothing methods for both functional time series and spatial data by extending trend filtering, a powerful nonparametric trend estimation technique for scalar data. We formulate the functional version of trend filtering by introducing L_2 -norm of the differences of adjacent trend functions. Through orthonormal basis expansion, we simplify the objective function to squared loss for coefficient vectors with grouped fused lasso penalty, and develop an efficient iteration algorithm for optimization. The tuning parameter in the proposed method is selected via cross validation. We also consider an extension of the proposed algorithm to spatial functional data. The proposed methods are demonstrated by simulation studies and an application to two real world datasets.

Keywords: ADMM algorithm; group fused lasso; regularized estimation; spatial functional data; trend filtering

*Corresponding author, Email: tom-w9@g.ecc.u-tokyo.ac.jp

1 Introduction

Due to advances in measurement devices and data storage resources, it is nowadays possible to observe functions as realizations of random experiments and thus functional data analysis (FDA) has expanded rapidly in recent decades. Functional versions for many branches of statistics have been provided, for example, in Ramsay (2004), Kokoszka and Reimherr (2017) and Horváth and Kokoszka (2012).

The conventional techniques of FDA for independent functional data have been recently extended to dependent situations (both time series and spatial cases). In fact, for functional time series data, standard stationary models for numerical data have been extended to functional settings (e.g. Besse et al., 2000; Klepsch and Klüppelberg, 2017; Klepsch et al., 2017; Hörmann et al., 2013) and theoretical properties have also been widely investigated (e.g. Bosq, 2000; Aue and Klepsch, 2017; Spangenberg, 2013; Aue et al., 2017; Kühnert, 2020; Cerovecki et al., 2019). On the other hand, effective estimation methods of functional trend under non-stationary situations are not well developed despite their importance in real applications. van Delft et al. (2018) addressed a framework for locally stationary functional times series, but its flexibility as trend estimation seems limited. Another existing approach is using functional principal component (FPC) analysis for dimension reduction and then applying standard time series analysis for the FPC scores (Hyndman and Ullah, 2007; Hyndman and Shang, 2009; Aue et al., 2015). Moreover, some dynamic versions of FPC that account for serial dependence are also considered (e.g. Gao et al., 2019; Hörmann et al., 2015; Panaretos and Tavakoli, 2013). Regarding spatial functional data, while spatial interpolation methods under spatial stationary have been developed (e.g. Giraldo et al., 2011; Nerini et al., 2010), there are some attempts to estimate non-stationary spatial trend determined by some external covariates (e.g. Caballero et al., 2013; Menafoglio et al., 2013, 2016). However, flexible estimation methods for spatially varying trend are not considered very much.

Although many useful tools are available for FDA, to the best of our knowledge, effective approaches for recovering time series or spatially varying trend are still scarce. In particular, the flexibility of existing methods may be limited; they do not necessarily handle possible

abrupt changes of the trend, which naturally arises the need of locally adaptive smoothing methods. For univariate time series, trend filtering (Kim et al., 2009; Tibshirani et al., 2014) is recognized as a powerful tool for locally adaptive trend estimation. Additionally, Wang et al. (2016) extended trend filtering to spatial data, which enables us to estimate spatial trend with abrupt changes revealed.

In this work, we provide an effective local smoothing method for both time series and spatial functional data by extending trend filtering for scalar data. Combining L_2 -loss for the true functions and a L_2 -norm penalty term for the finite order differences in functional trend functions, we successfully define the objective function for functional trend filtering. To solve the optimization problem, we expand the functional data and the functional trend via orthogonal basis functions. This results in an objective function similar to one for the group fused lasso (Alaíz et al., 2013), a mixture of the fused lasso (Tibshirani et al., 2005) and the grouped lasso (Yuan and Lin, 2006; Lounici et al., 2011; Tibshirani, 1996). We then develop an iteration algorithm based on the idea of ADMM (Boyd et al., 2011; Ramdas and Tibshirani, 2016), in which each updating procedure can be easily carried out. We also consider functional trend filtering for spatial functional data by generalizing the work by Wang et al. (2016). As for the tuning parameter selection, we simply suggest using cross validation, which is fairly feasible owing to the efficient optimization algorithm.

The remainder of the paper is organized as follows. Section 2 offers a brief review of trend filtering and its periphery, which is deeply related to our work. In Section 3, we present the proposed method, functional trend filtering, for both functional time series and spatial data, and describe the algorithm to carry out the proposed method. In Section 4, we compare the proposed method with some existing approaches through simulation studies. Finally, in Section 5, we apply the proposed method to functional time series (fertility rates as a function of age in each year) and functional spatial data (the number of confirmed COVID-19 cases as a function of day in Japanese prefectures).

2 Trend filtering for scalar data

Before describing the proposed method for functional data, we first briefly review trend filtering known as a powerful tool for locally adaptive smoothing for scalar data. Let y_1, \dots, y_n be a sequence of observations, and we are interested in denoising the observations to estimate the underlying true trend denoted by $\beta = (\beta_1, \dots, \beta_n)^\top$. The k th order trend filtering (Kim et al., 2009; Tibshirani et al., 2014) is defined as the minimizer of the following objective function:

$$\frac{1}{2} \sum_{t=1}^n (y_t - \beta_t)^2 + \lambda \sum_{t=1}^{n-k-1} |\Delta_t^{(k)} \beta|, \quad (1)$$

where $\lambda \geq 0$ is a tuning parameter which controls the trade-off between the fit to the observed data and smoothing the trend estimation. Here $\Delta_t^{(k)}$ is the t th row vector of the k th order discrete difference operator matrix $\Delta^{(k)}$ defined as

$$\Delta^{(k)} := \begin{cases} D^{(0)} & \text{for } k = 0, \\ D^{(k)} \Delta^{(k-1)} & \text{for } k \geq 1, \end{cases}$$

where $D^{(k)}$ is the following $(n - k - 1) \times (n - k)$ matrix:

$$D^{(k)} := \begin{pmatrix} 1 & -1 & 0 & \dots & 0 & 0 \\ 0 & 1 & -1 & \dots & 0 & 0 \\ \vdots & \vdots & \vdots & \ddots & \vdots & \vdots \\ 0 & 0 & 0 & \dots & 1 & -1 \end{pmatrix}$$

For example, (1) with $k = 0$ reduces to the same form of fused lasso (Tibshirani et al., 2005) and the penalty term makes many differences to zero exactly and leave others nonzero values, leading to piece-wise constant estimation of β . In general, sparsity of β under k th order discrete difference operator matrix suggests that the estimated components have a specific k th order piece-wise polynomial structure (Tibshirani et al., 2014). While trend filtering is locally adaptive estimator defined by a regularization problem with nonsmooth penalty term, it is still computationally efficient owing to its convexity.

The aforementioned trend filtering is also applicable to spatial data (Wang et al., 2016). Let $V = \{1, \dots, n\}$ be a set of sample index, which can be regard as vertex of graph

$G = (V, E)$. Here $E = \{e_1, \dots, e_m\}$ is a set of undirected edges according to the spatial adjacent structure, where $e_h \in V \times V$ for $h = 1, \dots, m$ and m is the total number of adjacency relationships. For example, $e_h = (i, j)$ means that i th and j th locations are adjacent. Let $\Delta^{(0)} \in \{1, 0, -1\}^{m \times n}$ be the oriented incidence matrix of the graph G , that is, $\Delta_{hi}^{(0)} = 1$, $\Delta_{hj}^{(0)} = -1$ and the other elements in the h th row vector of $\Delta^{(0)}$ is 0 if $e_h = (i, j)$. We then define

$$\Delta^{(k+1)} := \begin{cases} (\Delta^{(1)})^\top \Delta^{(k)} : n \times n \text{ matrix} & (\text{for even } k), \\ \Delta^{(1)} \Delta^{(k)} : m \times n \text{ matrix} & (\text{for odd } k). \end{cases}$$

This $\Delta^{(k)}$ is hereinafter referred to as the k th order graph difference operator matrix. The k th order spatial trend filtering estimate is obtained as the minimizer of the following function:

$$\frac{1}{2} \sum_{i=1}^n (y_i - \beta_i)^2 + \lambda \|\Delta^{(k)} \beta\|_1,$$

where λ is a tuning parameter. We remark it is also a form of fused lasso and accordingly it can be solved by basic convex optimization algorithms. Wang et al. (2016) discusses the computational aspect in detail. Notably, the penalty term encourages sparsity in graph differences in trend, which yields a piece-wise polynomial nature of the estimator as the original trend filtering (1).

3 Functional trend filtering

3.1 *Settings and objective function*

Let (Ω, \mathcal{A}, P) be an arbitrary probability space. The space $L^2(\mathcal{X})$ is defined as the set of all real valued square integrable functions on a compact set $\mathcal{X} \subset \mathbb{R}$. It is a Hilbert space with norm $\|f\|_{L^2} = (\int_{\mathcal{X}} f^2(x) dx)^{\frac{1}{2}}$, which is induced by the inner product $\langle f, g \rangle = \int_{\mathcal{X}} f(x)g(x) dx$ for $f, g \in L^2(\mathcal{X})$. We consider a serially indexed collection $\{Y_t(\cdot) : t = 1, \dots, n\}$ of random functions defined on the same probability space: $Y_t : \Omega \rightarrow L^2(\mathcal{X})$ is a measurable map. $\{y_t(\cdot) : t = 1, \dots, n\}$ denote a set of observed functions. We are interested in the estimation

of $\beta_t = E[Y_t]$, trend function on the period t . To estimate $\beta = (\beta_1, \dots, \beta_n)^\top \in (L^2(\mathcal{X}))^n$, we propose the k th order *functional trend filtering* defined as

$$\begin{aligned}\widehat{\beta}^{\text{TF}} &= \underset{\beta}{\text{argmin}} \left[\frac{1}{2} \sum_{t=1}^n \int_{\mathcal{X}} \{y_t(x) - \beta_t(x)\}^2 dx + \lambda \sum_{t=1}^{n-k-1} \left[\int_{\mathcal{X}} \left\{ \Delta_t^{(k)} \beta(x) \right\}^2 dx \right]^{1/2} \right] \quad (2) \\ &= \underset{\beta}{\text{argmin}} \left\{ \frac{1}{2} \sum_{t=1}^n \|y_t - \beta_t\|_{L^2}^2 + \lambda \sum_{t=1}^{n-k-1} \|\Delta_t^{(k)} \beta\|_{L^2} \right\},\end{aligned}$$

where $\lambda > 0$ is a tuning parameter and $\Delta_t^{(k)}$ is the t th row vector of the k th order difference operator matrix $\Delta^{(k)}$. For instance, if $k = 0$, the penalty term is $\sum_{t=1}^{n-1} \|\beta_t - \beta_{t+1}\|_{L^2}$, which can be regarded as the functional version of the group fused lasso (Alaíz et al., 2013). Henceforth, we have to solve the functional version of the group fused lasso for any order, desiring that some elements of $\{\Delta_t^{(k)} \widehat{\beta}^{\text{TF}} : t = 1, \dots, n-k-1\}$ are set to zero.

Since random functions are infinite dimensional and difficult to handle, we first prepare L orthonormal basis functions $\{\phi_\ell : \ell = 1, \dots, L\}$ on $L^2(\mathcal{X})$, which satisfy

$$\langle \phi_\ell, \phi_{\ell'} \rangle = \begin{cases} 1 & \text{if } \ell = \ell', \\ 0 & \text{otherwise.} \end{cases}$$

Then using the approximate expansions $y_t(x) \approx \sum_{\ell=1}^L z_{t\ell} \phi_\ell(x)$ and $\beta_t(x) \approx \sum_{\ell=1}^L b_{t\ell} \phi_\ell(x)$ with $z_{t\ell} = \langle y_t, \phi_\ell \rangle$ and $b_{t\ell} = \langle \beta_t, \phi_\ell \rangle$ for all t and ℓ , we reduce the problem (2) to minimization of the objective function

$$\frac{1}{2} \sum_{t=1}^n \sum_{\ell=1}^L (z_{t\ell} - b_{t\ell})^2 + \lambda \sum_{t=1}^{n-k-1} \left[\sum_{\ell=1}^L (\Delta_t^{(k)} \mathbf{b}_\ell)^2 \right]^{1/2}$$

with respect to $\mathbf{b}_\ell = (b_{1\ell}, \dots, b_{n\ell})^\top \in \mathbb{R}^n$. Define $B = (\mathbf{b}_1, \dots, \mathbf{b}_L)$ and $\mathbf{z}_\ell = (z_{1\ell}, \dots, z_{n\ell})^\top$.

Then, the above objective function can be further rewritten as

$$\frac{1}{2} \sum_{\ell=1}^L \|\mathbf{z}_\ell - \mathbf{b}_\ell\|_2^2 + \lambda \sum_{t=1}^{n-k-1} \|\Delta_t^{(k)} B\|_2, \quad (3)$$

where $\|\cdot\|$ denotes the ℓ_2 norm. Focusing on the second term, we notice it is a mixture of k th order fused lasso type penalty and grouped lasso type penalty. Alaíz et al. (2013) extended group lasso to a fused setting and addressed the solution, but the order of fusion is limited to 0; namely, the penalty is defined as the sum of ℓ_2 norm of 0th order differences.

Both $\|\cdot\|_2^2$ and $\|\cdot\|_2$ are convex functions and $\|\mathbf{z}_\ell - \mathbf{b}_\ell\|_2^2$ is differentiable with respect to \mathbf{b}_ℓ , but $\|\Delta_t^{(k)} B\|_2$ is not separable, namely, it cannot be represented as sum of the univariate convex function of each $b_{t\ell}$. Thus it is not straightforward to efficiently optimize the objective function with a general value of k .

3.2 Optimization

For notational simplicity, we use Δ instead of $\Delta^{(k)}$ in what follows. To optimize (3), we first introduce two unit vectors, $\mathbf{e}_t^a \in \mathbb{R}^{n-k-1}$ and $\mathbf{e}_t^b \in \mathbb{R}^L$, whose only t th and ℓ th elements are 1, respectively, and the other elements are 0.

Note that the ℓ th component of $\Delta_t B$ is $\Delta_t \mathbf{b}_\ell$. Since $\mathbf{e}_\ell^b \Delta_t B = \mathbf{e}_t^a \Delta \mathbf{b}_\ell$, we rewrite the optimization of (3) with respect to $\{\mathbf{b}_\ell\}$ as the following constraint optimization problem:

$$\begin{aligned} \operatorname{argmin}_{\{\mathbf{a}_t\}, \{\mathbf{b}_\ell\}} & \left\{ \frac{1}{2} \sum_{\ell=1}^L \|\mathbf{z}_\ell - \mathbf{b}_\ell\|_2^2 + \lambda \sum_{t=1}^{n-k-1} \|\mathbf{a}_t\|_2 \right\} \\ \text{subject to} & \quad \mathbf{e}_\ell^b \mathbf{a}_t = \mathbf{e}_t^a \Delta \mathbf{b}_\ell \quad (\ell = 1, \dots, L \text{ and } t = 1, \dots, n-k-1). \end{aligned}$$

Note that such transformation of the objective function is very similar to alternating direction method of multipliers (ADMM) algorithm (Boyd et al., 2011; Ramdas and Tibshirani, 2016), which breaks the problem into smaller pieces that are easier to deal with. We then define an augmented Lagrangian function

$$\begin{aligned} L_\rho(\{\mathbf{a}_t\}, \{\mathbf{b}_\ell\}, \{\mathbf{u}_t\}) := & \frac{1}{2} \sum_{\ell=1}^L \|\mathbf{z}_\ell - \mathbf{b}_\ell\|_2^2 + \lambda \sum_{t=1}^{n-k-1} \|\mathbf{a}_t\|_2 \\ & + \sum_{t=1}^{n-k-1} \sum_{\ell=1}^L u_{t\ell} (\mathbf{e}_t^a \Delta \mathbf{b}_\ell - \mathbf{e}_\ell^b \mathbf{a}_t) + \frac{\rho}{2} \sum_{t=1}^{n-k-1} \sum_{\ell=1}^L (\mathbf{e}_t^a \Delta \mathbf{b}_\ell - \mathbf{e}_\ell^b \mathbf{a}_t)^2, \end{aligned} \quad (4)$$

where $\{u_{t\ell}\}_{t,\ell}$ is Lagrange multipliers and $\rho > 0$ controls the influence of the violation of equality constraint. Since there is no apparent closed form solution for \mathbf{b}_ℓ minimizing the objective function L_ρ , we develop an iterative algorithm outlined in Algorithm 1, where the derivation is deferred to the Appendix.

From the existing theory of ADMM algorithm, the choice of ρ is related only to the speed of convergence of the algorithm without affecting the final estimates (see Boyd et al.,

2011; Fukushima, 1992; He et al., 2000, in detail). In our implementation, we simply set $\rho = 0.1$.

Using the coefficients $\widehat{\mathbf{b}}_\ell^{\text{TF}}$ computed by the procedure, we obtain the function

$$\widehat{\beta}_t^{\text{TF}}(x) = \sum_{\ell=1}^L \widehat{b}_{t,\ell}^{\text{TF}} \phi_\ell(x)$$

for $t = 1, \dots, n$, which is the estimator of the trend.

As an alternative smoother, we construct a simplified version of the trend estimation, defined as

$$\widehat{\beta}^{\text{HP}} = \underset{\beta \in (L^2(\mathcal{X}))^n}{\operatorname{argmin}} \frac{1}{2} \sum_{t=1}^n \int_{\mathcal{X}} (y_t(x) - \beta_t(x))^2 dx + \lambda \sum_{t=1}^{n-k-1} \int_{\mathcal{X}} \{\Delta_t \beta(x)\}^2 dx, . \quad (5)$$

The difference between (5) and (2) is the penalty in the second term; the penalty in (5) is the squared value of the L^2 -norm used in (2). Note that the estimator defined in (5) can be regarded as an extension of Hodrick-Prescott (HP) filter (Hodrick and Prescott, 1997) for scalar data. Although the use of squared norm penalty does not produce sparsity in the differences, the notable property of (5) is its ease of computation. In fact, by expanding (5) via orthonormal functions, we have the following approximation of the objective function:

$$\frac{1}{2} \sum_{\ell=1}^L \|\mathbf{z}_\ell - \mathbf{b}_\ell\|_2^2 + \lambda \sum_{t=1}^{n-k-1} \sum_{\ell=1}^L (\Delta_t \mathbf{b}_\ell)^2, \quad (6)$$

which yields the closed form solution given by

$$\widehat{\mathbf{b}}_\ell^{\text{HP}} = \left(I_n + 2 \sum_{t=1}^{n-k-1} \lambda \Delta_t^\top \Delta_t \right)^{-1} \mathbf{z}_\ell, \quad \ell = 1, \dots, L.$$

In some situations, it works better than functional trend filtering. (Details are given in Section 4.)

Finally, we discuss the choice of tuning parameter λ . In practice, the value of λ used for filtering is determined by K -fold cross validation, where we divide the dataset into K subsets by extracting every K th function. As the estimate of \mathbf{b}_t in a validation dataset, we take the midpoint of \mathbf{b}_{t-1} and \mathbf{b}_{t+1} after smoothing.

Algorithm 1 (Functional trend filtering)

Input: z_1, \dots, z_L (coefficient vector), Δ (difference operator), $\varepsilon_0, \varepsilon_1$ (tolerance level)

Initialization: $b_{t\ell}^{(0)}, a_{t\ell}^{(0)}, u_{t\ell}^{(0)}$

while $\sum_{\ell=1}^L \|b_{\ell}^{(v+1)} - b_{\ell}^{(v)}\|_2 \geq \varepsilon_0$ **do**

< update b_{ℓ} >

for $\ell = 1, \dots, L$ **do**

$b_{\ell}^{(v+1)} \leftarrow (I + \rho \Delta^T \Delta)^{-1} \{z_{\ell} - \sum_t u_{t\ell}^{(v)} (\mathbf{e}_t^a \Delta)^T + \rho \sum_t (\mathbf{e}_t^a \Delta)^T \mathbf{e}_{\ell}^b a_t^{(v)}\}$

end for

< update a_t >

for $t = 1, \dots, n - k - 1$ **do**

$\hat{w}_0 = a_t^{(v)} \in \mathbb{R}^L, s_0 \leftarrow 1, j \leftarrow 0, \eta \leftarrow 1$

while $\|w_{j+1} - w_j\|_2 \geq \varepsilon_1$ **do**

$w_{j+1} \leftarrow S_{\lambda} \{(1 - \rho) \hat{w}_j + \rho \sum_{\ell} \mathbf{e}_{\ell}^{b\top} (\mathbf{e}_t^a \Delta b_{\ell}^{(v+1)} + \rho^{-1} u_{t\ell}^{(v)})\}$

with $S_{\lambda}(\mathbf{s}) := \max(0, 1 - \lambda / \|\mathbf{s}\|_2) \mathbf{s}$

$s_{j+1} \leftarrow (1 + \sqrt{1 + 4s_j^2}) / 2$

$\hat{w}_{j+1} \leftarrow w_{j+1} + (s_j - 1)(w_{j+1} - w_j) / s_{j+1}$

end while

$a_t^{(v+1)} \leftarrow w_j$

end for

< update $u_{t\ell}$ >

for $t = 1, \dots, n - k - 1$ and $\ell = 1, \dots, L$ **do**

$u_{t\ell}^{(v+1)} \leftarrow u_{t\ell}^{(v)} + \rho (\mathbf{e}_t^a \Delta b_{\ell} - \mathbf{e}_{\ell}^b a_t)$

end for

end while

3.3 Extension to spatial functional data

Let $G = (V, E)$ be the graph with vertices $V = \{1, \dots, n\}$ and undirected edges $E = \{e_1, \dots, e_m\}$, representing spatial adjacent structure as introduced in Section 2. Let $\{Y_i(\cdot) : 1, \dots, n\}$ be random functions on the vertices, which take values in the space $L^2(\mathcal{X})$ on a compact set $\mathcal{X} \subset \mathbb{R}$. Suppose that $E[Y_i(x)] = \beta_i(x)$ for $i = 1, \dots, n$ and we are interested in the estimation of $\beta_i(x)$. Let $\Delta^{(k)}$ be k th order graph difference operator matrix defined in Section 2. We propose the k th order *functional trend filtering on graph* to estimate $\beta = (\beta_1, \dots, \beta_n)^\top$ by

$$\widehat{\beta}^{\text{TF}} = \underset{\beta \in (L^2(\mathcal{X}))^n}{\operatorname{argmin}} \frac{1}{2} \sum_{i=1}^n \int_{\mathcal{X}} (y_i(x) - \beta_i(x))^2 dx + \lambda \sum_{p=1}^q \left[\int_{\mathcal{X}} \{\Delta_p^{(k)} \beta(x)\}^2 dx \right]^{1/2} \quad (7)$$

where $q = n$ if k is odd, $q = m$ otherwise. The penalty term quantifies how much β vary locally in the sense of k th order graph differences. We prepare L orthonormal basis functions $\phi(x)$ and approximate $y_i(x) \approx \sum_{\ell=1}^L z_{i\ell} \phi_\ell(x)$ and $\beta_i(x) \approx \sum_{\ell=1}^L b_{i\ell} \phi_\ell(x)$ with $z_{i\ell} = \langle y_i, \phi_\ell \rangle$ and $b_{i\ell} = \langle \beta_i, \phi_\ell \rangle$ for all i and ℓ .

In the following discussion in this section, we write Δ for $\Delta_p^{(k)}$. Define two standard unit vectors $\mathbf{e}_p^a \in \mathbb{R}^q$ and $\mathbf{e}_\ell^b \in \mathbb{R}^L$, whose only t th and ℓ th elements are 1, respectively, and the other elements are 0, and $\mathbf{b}_\ell = (b_{1\ell}, \dots, b_{n\ell})^\top \in \mathbb{R}^n$. Following the same logic as the previous section, we regard the problem to find (7) as a problem to get $\{\mathbf{b}_\ell\}$ minimizing an augmented Lagrangian, for a parameter $\rho > 0$,

$$\begin{aligned} L_\rho(\{\mathbf{a}_p\}, \{\mathbf{b}_\ell\}, \{\mathbf{u}_p\}) := & \frac{1}{2} \sum_{\ell=1}^L \|\mathbf{z}_\ell - \mathbf{b}_\ell\|_2^2 + \lambda \sum_{p=1}^q \|\mathbf{a}_p\|_2 \\ & + \sum_{p=1}^q \sum_{\ell=1}^L u_{p\ell} (\mathbf{e}_p^a \Delta \mathbf{b}_\ell - \mathbf{e}_\ell^b \mathbf{a}_p) + \frac{\rho}{2} \sum_{p=1}^q \sum_{\ell=1}^L (\mathbf{e}_p^a \Delta \mathbf{b}_\ell - \mathbf{e}_\ell^b \mathbf{a}_p)^2. \end{aligned}$$

To solve this problem, we can again utilize Algorithm 1. Using the acquired coefficients $\widehat{\mathbf{b}}_\ell^{\text{TF}}$ computed by the procedure, we obtain the function

$$\widehat{\beta}_i^{\text{TF}}(x) = \sum_{\ell=1}^L \widehat{b}_{i,\ell}^{\text{TF}} \phi_\ell(x),$$

for $i = 1, \dots, n$. This is the estimator of the proposed method.

As an alternative smoothing estimator, we also propose an estimator corresponding to (5) in time series setting, or, Laplacian regularization (Smola and Kondor, 2003) for univariate data,

$$\widehat{\beta}^{\text{HP}} = \underset{\beta \in (L^2(\mathcal{X}))^n}{\operatorname{argmin}} \frac{1}{2} \sum_{t=1}^n \int_{\mathcal{X}} (y_t(x) - \beta_t(x))^2 dx + \lambda \sum_{p=1}^q \int_{\mathcal{X}} \{\Delta_p \beta(x)\}^2 dx. \quad (8)$$

By treatment with the same approximation as the former section, we convert the problem into the optimization problem with objective function:

$$\frac{1}{2} \sum_{i=1}^n \sum_{\ell=1}^L (z_{i\ell} - b_{i\ell})^2 + \lambda \sum_{p=1}^q \sum_{\ell=1}^L (\Delta_p b_{\ell})^2.$$

For $\ell = 1, \dots, L$, the closed form solution is given by

$$\widehat{\mathbf{b}}_{\ell}^{\text{HP}} = \left(I_n + 2 \sum_{p=1}^q \lambda \Delta_p^{\top} \Delta_p \right)^{-1} \mathbf{z}_{\ell}.$$

Consequently, we obtain the estimator $\widehat{\beta}_i^{\text{HP}}(x) = \sum_{\ell=1}^L \widehat{b}_{i,\ell}^{\text{HP}} \phi_{\ell}(x)$ for $i = 1, \dots, n$.

4 Simulation Studies

We investigate the performance of the proposed methods together with existing ones through simulation studies. For $t = 1, \dots, n (= 50)$ and the domain $\mathcal{X} = [1, 120]$, we adopt the four scenarios of the true trend function:

- (1) Constant: $\beta_t(x) = 0$,
- (2) Smooth: $\beta_t(x) = 40 \sin\left(\frac{t+x}{12}\right)$,
- (3) Piecewise constant: $\beta_t(x) = 40\mathbb{I}_{\{0 < t \leq 10\}} + 40\mathbb{I}_{\{20 < t \leq 30\}} + 40\mathbb{I}_{\{40 < t \leq 50\}}$,
- (4) Varying smoothness: $\beta_t(x) = \frac{x}{3} \left\{ \sin\left(\frac{4t}{n} - 2\right) + 2 \exp\left(-30\left(\frac{4t}{n} - 2\right)^2\right) \right\}$,

which can be seen as a slight modification of scenarios adopted in simulation studies of local smoothing (e.g. Faulkner and Minin, 2018). The observed functional data is generated by adding $N(0, \sigma^2)$ noise at $H = 120$ points of x , namely, $x \in \{1, 2, \dots, H\}$. The smoothed version of the generated functional data under the four scenarios are shown in Figure 1.

In scenario (1), we examine the abilities of the methods to find the horizontal line in the presence of noise. In scenario (2), we investigate whether the adaptive methods extract the continuous curve from the noisy data. Scenario (3) unearths the capability of the methods to spot the sharp changes, the points of discontinuities, between intermittent straight horizontal lines. In scenario (4), we test the abilities to catch the trend when the smoothness of the process varies significantly due to a sharp peak in the middle as a function of t .

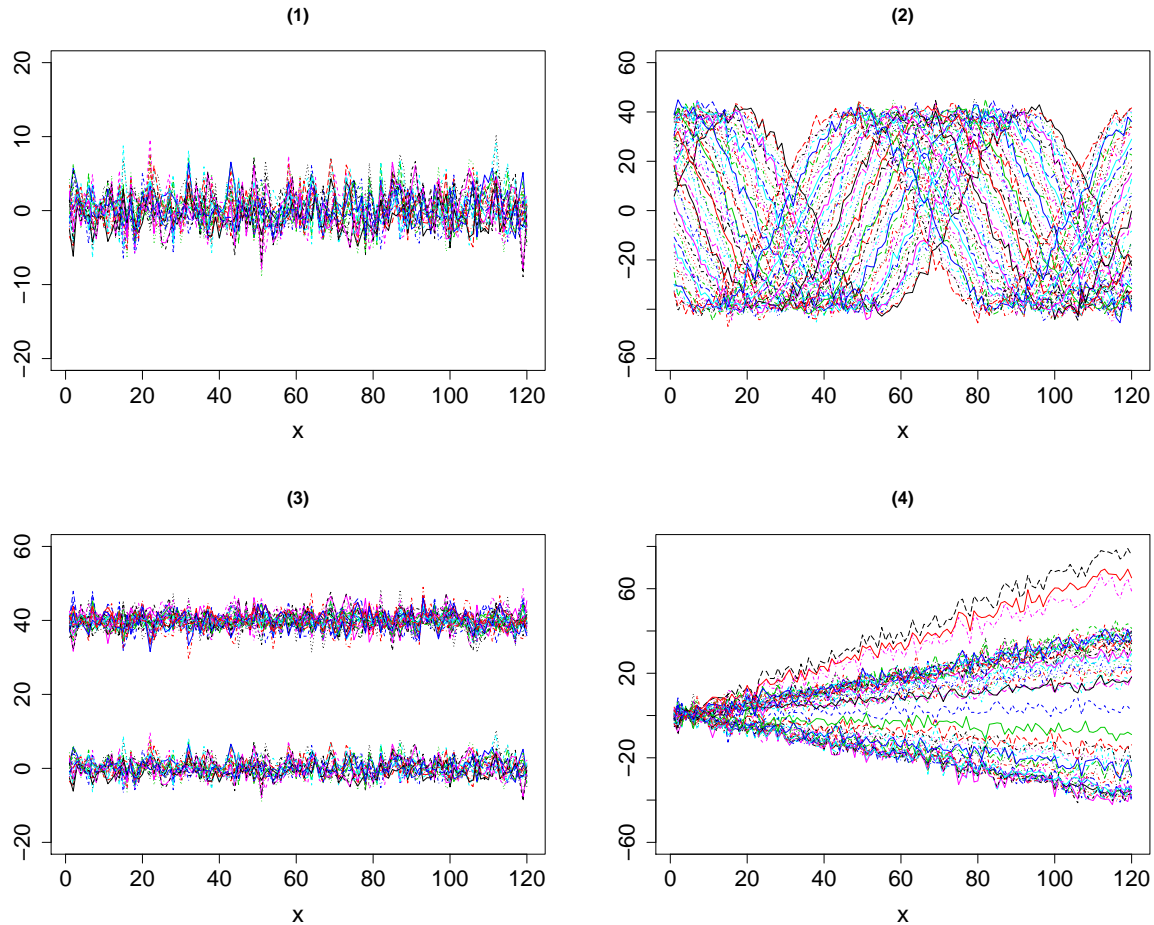


Figure 1: The simulated functional data under four scenarios with $\sigma = 5$, smoothed by FPC with five principle component functions.

For the simulated data, we apply the following four methods:

- **FTF**: The proposed functional trend filtering with $k \in \{0, 1, 2\}$.
- **FHP**: Functional HP filter with $k \in \{0, 1, 2\}$ used for setting the initial values of FTF.
- **FPC**: The standard functional principle component method using R package “fda.usc”.
- **DFPC**: The dynamic functional principle component method using R package “freadom.fda”.

Note that we used the estimated principle component functions by FPC as orthonormal functions for FTF and FHP with $L = 5$ (the number of principle functions) to allow comparison independent of basis functions, and selected the tuning parameter λ for FTF and FHP and window-size for DFPC through 10-fold cross-validation as explained in the end of Section 3.2. We search for the optimal value of λ from the space $[10^{-3}, 10^3]$ by checking 60 points equally spaced on a logarithmic scale in all scenarios and the optimal window-size from the set $\{1, \dots, 30\}$.

The estimated trend functions at $x = 80$ are presented in Figure 2. Based on 250 times repeated simulation, we also report the mean squared error (MSE), $(nH)^{-1} \sum_t \sum_x (\hat{\beta}_t(x) - \beta_t(x))^2$, in Table 1, where $\hat{\beta}_t(x)$ is the estimated trend functions. Overall, the proposed FTF tends to perform better than the other methods. Further, we can see from Figure 2 that both FPC and DFPC provide under-smoothed trend functions compared with FTF and FHP, which is related to the overall performance in terms of MSE reported in Table 1. Interestingly, the performance of FTF and FHP are quite different, although the only methodological difference is whether L^2 -norm or squared L^2 -norm is adopted in the penalty function. For example, in scenario (3), the performance of FHP is almost the same as that of FPC while FTF provides better results. This can be attributed to the fact that FHP does not have sparsity. Regarding the performance of FTF depending on k , it is observed that FTF with $k = 0$ provides the most accurate results in scenario (3) since the true trend admits a piecewise constant structure that FTF with $k = 0$ is considered to work well. In the other scenarios, however, the piecewise constant structure that FTF with $k = 0$ imposes seems rather limited, and the performance of FTF with $k = 1, 2$ is more appealing.

Finally, DFPC works better than FPC by successfully incorporating serial dependence, but its performance is worse than FTF, except for scenario 4 with the small noises.

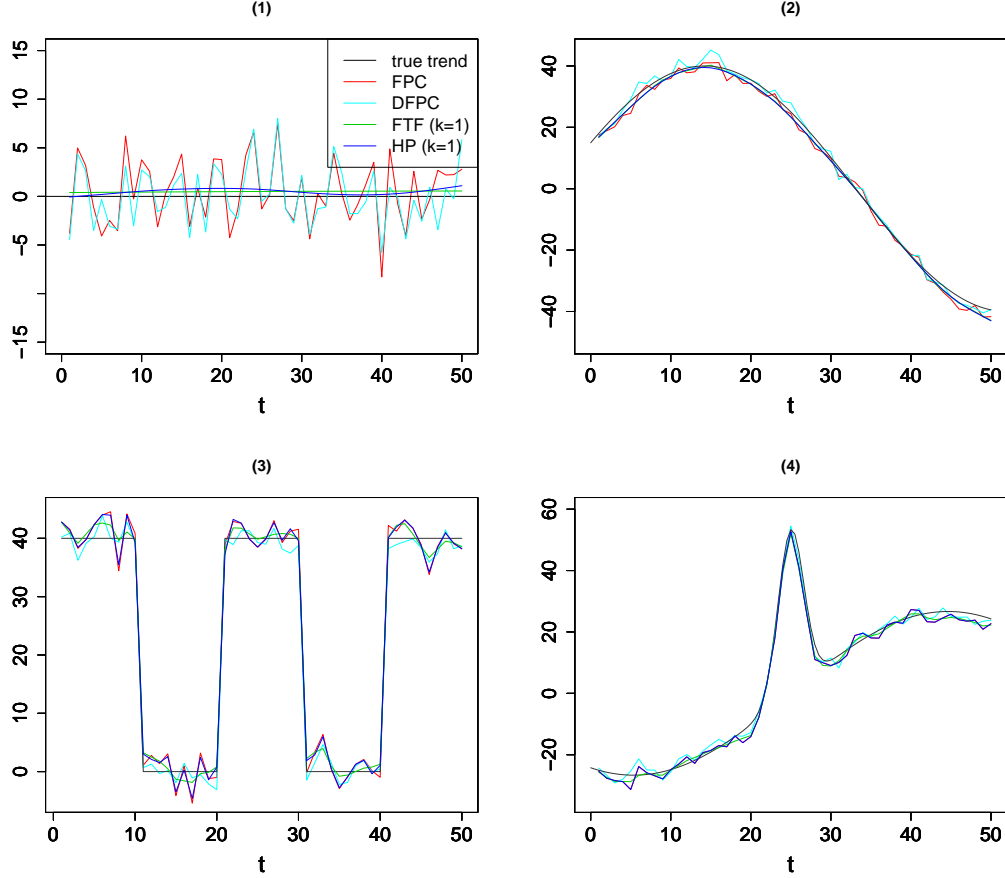


Figure 2: The fitted results of the four methods, FPC, DFPC, FTF ($k = 1$) and FHP ($k = 1$) at $x = 80$ under four scenarios with $\sigma = 5$.

5 Applications

5.1 Australian fertility rates

Fertility rates in Australia have been declining seriously as in other developed countries. We examine the data "Australiasmoothfertility", which is available from R package "rainbow". The original data, obtained from the Australian Bureau of Statistics, describes the age-

Table 1: MSE of functional trend filtering (FTF), functional HP filtering (FHP), functional principle component analysis (FPC) and dynamic FPC (DFPC) under four scenarios with $\sigma \in \{3, 5, 7\}$.

σ	method	Scenario			
		(1)	(2)	(3)	(4)
3	FTF ($k = 0$)	0.184	1.345	0.886	2.201
	FTF ($k = 1$)	0.252	0.912	1.352	2.201
	FTF ($k = 2$)	0.346	0.864	2.128	2.200
	FHP ($k = 0$)	0.184	1.287	2.107	2.188
	FHP ($k = 1$)	0.184	0.859	2.112	2.162
	FHP ($k = 2$)	0.185	0.796	2.139	2.084
	FPC	2.187	2.068	2.129	2.202
	DFPC	1.823	1.761	1.994	1.738
	FTF ($k = 0$)	0.507	2.984	2.205	4.492
	FTF ($k = 1$)	0.647	2.101	3.457	2.906
5	FTF ($k = 2$)	0.816	2.067	4.344	5.847
	FHP ($k = 0$)	0.503	2.745	5.518	5.811
	FHP ($k = 1$)	0.503	1.990	5.632	5.740
	FHP ($k = 2$)	0.503	1.872	5.745	5.525
	FPC	6.084	5.464	5.784	5.848
	DFPC	5.076	4.877	5.532	4.824
	FTF ($k = 0$)	0.998	5.168	3.890	5.798
	FTF ($k = 1$)	1.232	3.773	6.544	5.186
	FTF ($k = 2$)	1.671	3.853	8.276	6.979
	FHP ($k = 0$)	0.991	4.721	10.199	11.234
7	FHP ($k = 1$)	0.992	3.655	10.571	10.196
	FHP ($k = 2$)	0.992	3.486	11.035	8.062
	FPC	11.897	10.550	11.252	11.309
	DFPC	9.927	9.549	10.831	9.443

specific number of live births per 1000 females of ages 15, 16, ..., 49 from 1921 to 2006. The data is functional data and each function represents the age-specific number between 15 and 49 in a year. Fig 3 shows the curves with rainbow colors. The colors indicate that the oldest curve is red, the newest curve is purple and the others are colored in the same order as a rainbow.

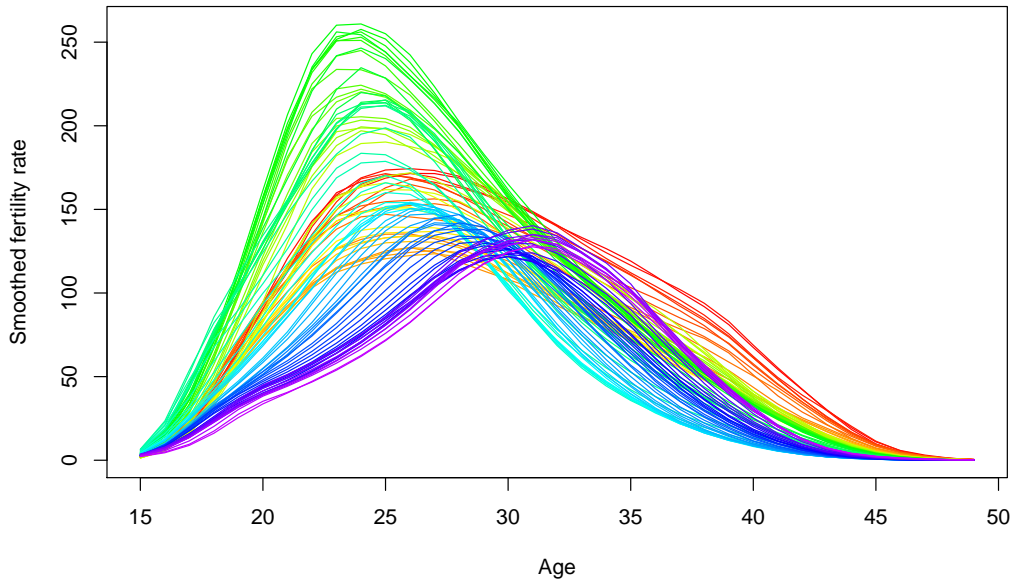


Figure 3: Age-specific Australian fertility rates curves for ages 15 to 49 observed from 1921 to 2006 (in the same order as the color in a rainbow).

We apply trend filtering to the functional data. The value of λ is selected by cross validation from candidates $\{5, 10, \dots, 50\}$. Figure 4 shows the number of births per 1000 females of ages 20 and 30 in all years and curves fitted by FPC and trend filtering. Figure 5 displays absolute values of 1st order differences and 2nd order differences in scores of the first principal component (PC1) between the years and their trend filtered versions. First, compared with FPC, the ability of trend filtering to serve as a smoother is confirmed from Figure 4. Next, in common between age 20 and 30 in Figure 4, we find abrupt changes in 1961 and 1972. After World War II, the fertility rate had increased until 1961, although

the first oral contraceptive pill was released in Australia in 1961. Furthermore, in 1972, the prime minister of Australia at that time abolished the 27.5 percent luxury tax on all contraceptives (McLennan, 1998). It increased the use of the pills especially among young people and the trends are reflected as the sharp change points in plots in Figure 4. Moreover, from the upper right plot in Figure 5, the structure in the sense of 1st order difference is considered to change at 40th and 51st points, around 1961 and 1972. The lower left plot suggests, in terms of 2nd order difference, the structure changes at 24th point (i.e. around 1945), implying that the trend of the fertility rate changed after the end of World War II. Owing to the sparsity in differences in trend, we easily detect those underlying events. In addition, since the detected points from the plots tend to be overlapped between $k = 1$ and 2 in Figure 5, trend filtering would be able to stably extract the turning points regardless of the order k . By contrast, we hardly find the structural properties of data from the original score of the principal component. Therefore, the result proves the ability of trend filtering to catch sharp changes.

5.2 *The number of COVID-19 cases in Japanese prefectures*

Infection with the novel COVID-19 has been spreading since 2020 and has brought about many deaths worldwide. Thus analyzing the situation becomes increasingly important. For instance, Tang et al. (2020) exploited some functional time series methods to analyze the COVID-19 data in the US. In this study, we investigate the number of people infected by COVID-19 by prefecture in Japan, which is available at <https://www3.nhk.or.jp/news/special/coronavirus/data-widget/>, and we scale the number by population of each prefecture available at <https://www.stat.go.jp/data/nihon/02.html>. Each prefecture is treated as a vertex on a graph, and when the prefectures are adjacent to each other, the connectivity of the graph is considered. We handle the number of infected people per million in each prefecture from January 16, 2020 to March 9, 2021, and regard them as functional data after smoothing. For example, Figure 6 illustrates the original data of the number of new cases of infections per million people and its functional data smoothed by FPC and 2nd order FTF in Tokyo in the period.

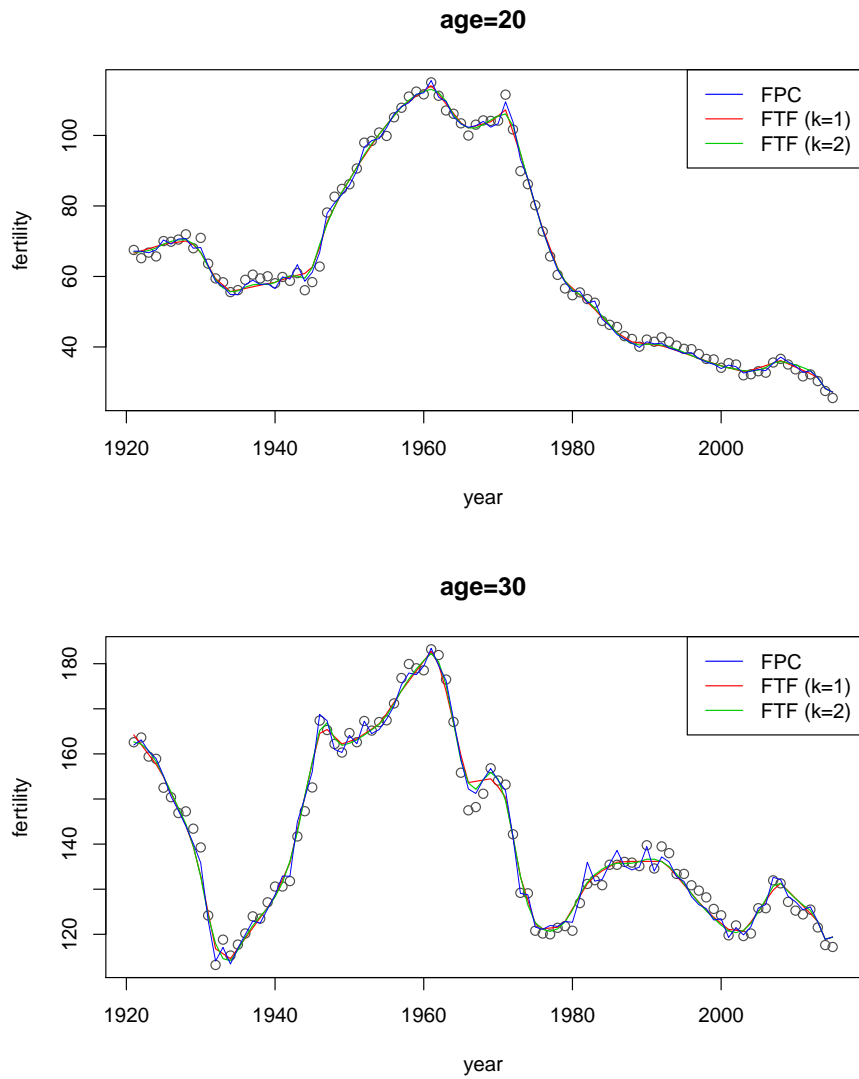


Figure 4: Round point: the number of births per 1000 females in all years. Blue curves: curves fitted by FPC. Red (green) curves: curves fitted by 1st (2nd) order FTF.

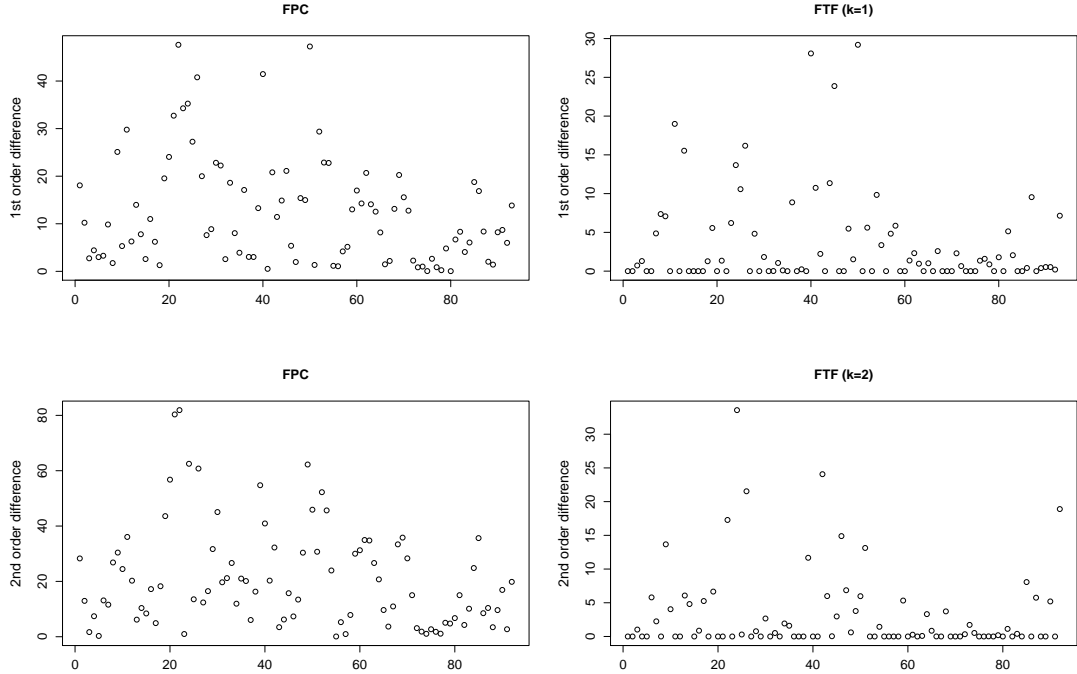


Figure 5: Top left: absolute values of 1st order differences in scores of PC1. Top right: absolute values of 1st order differences in the trend filtered scores. Bottom left: absolute values of 2nd order differences in the scores. Top right: absolute values of 2nd order differences in the trend filtered scores.

The observed data on 395th day are shown in the upper left panel in Figure 7. We plot the data fitted by FPC in the upper right panel and FTF with $k = 2$ in the lower left panel, where the value of λ is selected by the same way in Section 5.1. We also applied FTF with $k = 1$, but the result as almost the same, thereby we do not display it here.

For a qualitative visual analysis, although FTF is smooth trend better than FPC, whose result is still jagged, as we expected, trend filtering is more effective in that it spots an outstanding (dark colored) prefecture, Tokyo. Evidently, FTF is able to localize its estimates around strong inhomogeneous spikes, which implies that it is able to detect the event or spot of interest.

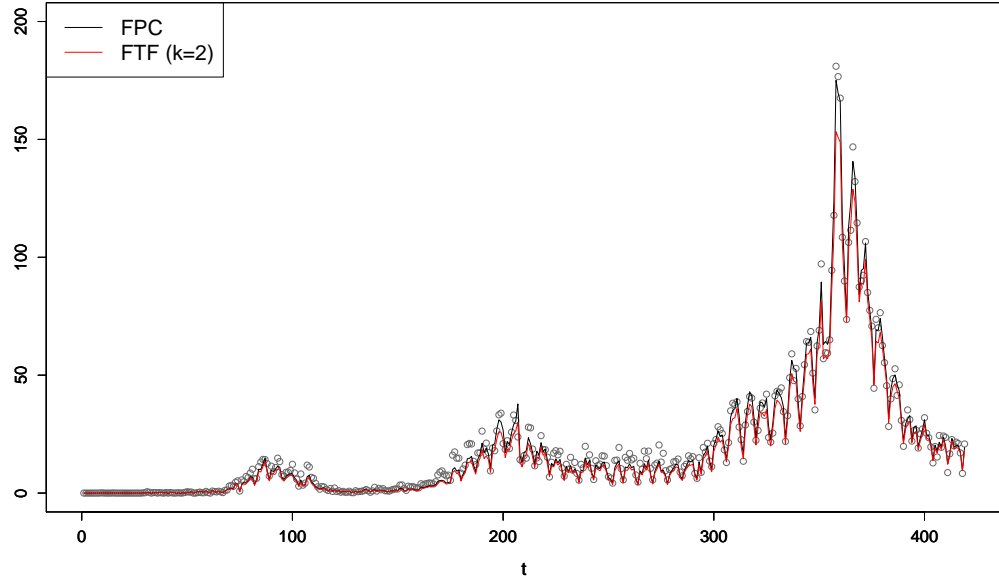


Figure 6: Round points: the number of new cases of infections per million in Tokyo for 419 days (from January 16, 2020 to March 9, 2021). Black (red) line: its functional data smoothed by FPC (2nd order FTF).

6 Concluding remarks

In this paper, we proposed a functional version of the locally adaptive smoothing technique known as trend filtering for smoothing functional time series and spatial data. We developed an efficient optimization algorithm to obtain trend estimation and discussed the choice of tuning parameter. Through simulation and empirical studies, we demonstrated the superiority of the proposed method to existing principle component methods. The optimization problem for computing the proposed method can be regarded as generalization and combination of grouped and fused lasso estimation, thereby it would be interesting to apply the proposed optimization techniques to other statistical problems, for example, regression analysis with complicated sparsity-inducing penalty functions.

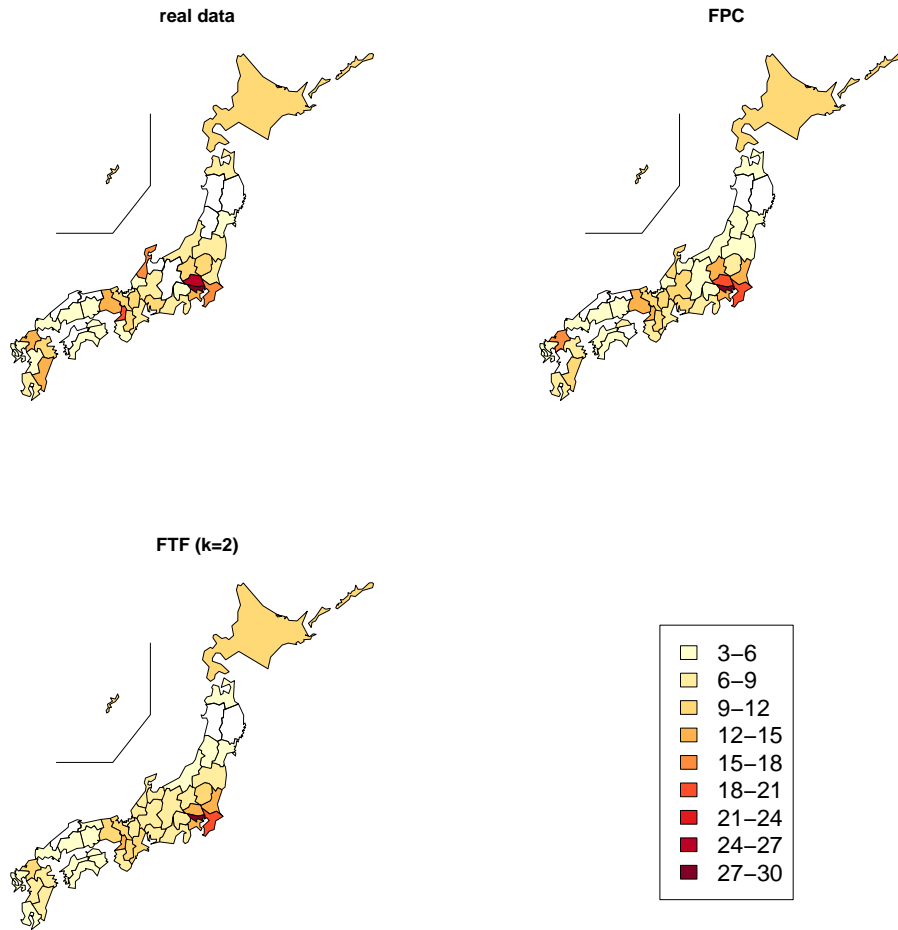


Figure 7: Top left: real data. Top right: FPC. Bottom left: 2nd order FTF.

Acknowledgment

This research is partially supported by Japan Society for Promotion of Science (KAKENHI) grant numbers 18H03628 and 21H00699.

Appendix

Derivation of Algorithm 1

We here provide the detailed derivation of each step in Algorithm 1.

- (Update of \mathbf{b}_ℓ) For $\ell = 1, \dots, L$, given $u_{t\ell}$ and \mathbf{a}_t , \mathbf{b}_ℓ can be updated by using the minimizer of

$$\frac{1}{2} \sum_{\ell=1}^L \|\mathbf{z}_\ell - \mathbf{b}_\ell\|_2^2 + \sum_t \sum_\ell u_{t\ell} (\mathbf{e}_t^a \Delta \mathbf{b}_\ell - \mathbf{e}_\ell^b \mathbf{a}_t) + \frac{\rho}{2} \sum_t \sum_\ell (\mathbf{e}_t^a \Delta \mathbf{b}_\ell - \mathbf{e}_\ell^b \mathbf{a}_t)^2,$$

which is a quadratic function of \mathbf{b}_ℓ . Since its derivative with respect to \mathbf{b}_ℓ is given by

$$(I + \rho \Delta^\top \Delta) \mathbf{b}_\ell - \mathbf{z}_\ell + \sum_t u_{t\ell} (\mathbf{e}_t^a \Delta)^\top - \rho \sum_t (\mathbf{e}_t^a \Delta)^\top \mathbf{e}_\ell^b \mathbf{a}_t,$$

the minimizer can be obtained as

$$\mathbf{b}_\ell \leftarrow (I + \rho \Delta^\top \Delta)^{-1} \left\{ \mathbf{x}_\ell - \sum_t u_{t\ell} (\mathbf{e}_t^a \Delta)^\top + \rho \sum_t (\mathbf{e}_t^a \Delta)^\top \mathbf{e}_\ell^b \mathbf{a}_t \right\}.$$

- (Update of \mathbf{a}_t) For $t = 1, \dots, n - k - 1$, given $u_{t\ell}$ and \mathbf{b}_ℓ , \mathbf{a}_t can be updated as the minimizer of

$$\lambda \sum_{t=1}^{n-k-1} \|\mathbf{a}_t\|_2 + \frac{\rho}{2} \sum_t \sum_\ell \left(\mathbf{e}_t^a \Delta \mathbf{b}_\ell - \mathbf{e}_\ell^b \mathbf{a}_t + \frac{u_{t\ell}}{\rho} \right)^2 \quad (9)$$

Because the objective function (6) is non differentiable due to the presence of the $\|\mathbf{a}_t\|_2$, we deal with the problem by a proximal method. We denote the first term (non-smooth part) by f_{nsm} and the second part (smooth part) by f_{sm} . Since f_{sm} is convex and $\nabla_{\mathbf{a}_t} f_{sm}$ is Lipschitz continuous with constant 1, FISTA (fast iterative shrinkage-thresholding algorithm), first presented by Beck and Teboulle (2009), can be applied. Remarking that, in general, the proximity operator of the ℓ_2 norm ($\|\cdot\|_2 : \mathbb{R}^d \rightarrow \mathbb{R}$, $d \in \mathbb{N}$), known as soft thresholding operator, is $S_\lambda(\mathbf{s}) = \max(0, 1 - \lambda/\|\mathbf{s}\|_2) \mathbf{s}$ for $\mathbf{s} \in \mathbb{R}^d$, we get the updating step given in Algorithm 1.

- (Update of $u_{t\ell}$) For $\ell = 1, \dots, L$ and $t = 1, \dots, n - k - 1$, given \mathbf{b}_ℓ , \mathbf{a}_t and $u_{t\ell}^*$ (current value of $u_{t\ell}$), $u_{t\ell}$ can be updated as $u_{t\ell} \leftarrow u_{t\ell}^* + \rho(\mathbf{e}_t^a \Delta \mathbf{b}_\ell - \mathbf{e}_\ell^b \mathbf{a}_t)$.

References

Alaíz, C. M., A. Barbero, and J. R. Dorronsoro (2013). Group fused lasso. In *International Conference on Artificial Neural Networks*, pp. 66–73. Springer.

Aue, A., L. Horváth, and D. F. Pellatt (2017). Functional generalized autoregressive conditional heteroskedasticity. *Journal of Time Series Analysis* 38(1), 3–21.

Aue, A. and J. Klepsch (2017). Estimating functional time series by moving average model fitting. *arXiv preprint arXiv:1701.00770*.

Aue, A., D. D. Norinho, and S. Hörmann (2015). On the prediction of stationary functional time series. *Journal of the American Statistical Association* 110(509), 378–392.

Beck, A. and M. Teboulle (2009). A fast iterative shrinkage-thresholding algorithm for linear inverse problems. *SIAM journal on imaging sciences* 2(1), 183–202.

Besse, P. C., H. Cardot, and D. B. Stephenson (2000). Autoregressive forecasting of some functional climatic variations. *Scandinavian Journal of Statistics* 27(4), 673–687.

Bosq, D. (2000). *Linear processes in function spaces: theory and applications*, Volume 149. Springer Science & Business Media.

Boyd, S., N. Parikh, and E. Chu (2011). *Distributed optimization and statistical learning via the alternating direction method of multipliers*. Now Publishers Inc.

Caballero, W., R. Giraldo, and J. Mateu (2013). A universal kriging approach for spatial functional data. *Stochastic environmental research and risk assessment* 27(7), 1553–1563.

Cerovecki, C., C. Francq, S. Hörmann, and J.-M. Zakoian (2019). Functional garch models: the quasi-likelihood approach and its applications. *Journal of econometrics* 209(2), 353–375.

Faulkner, J. R. and V. N. Minin (2018). Locally adaptive smoothing with markov random fields and shrinkage priors. *Bayesian analysis* 13(1), 225.

Fukushima, M. (1992). Application of the alternating direction method of multipliers to separable convex programming problems. *Computational Optimization and Applications* 1(1), 93–111.

Gao, Y., H. L. Shang, and Y. Yang (2019). High-dimensional functional time series forecasting: An application to age-specific mortality rates. *Journal of Multivariate Analysis* 170, 232–243.

Giraldo, R., P. Delicado, and J. Mateu (2011). Ordinary kriging for function-valued spatial data. *Environmental and Ecological Statistics* 18(3), 411–426.

He, B., H. Yang, and S. Wang (2000). Alternating direction method with self-adaptive penalty parameters for monotone variational inequalities. *Journal of Optimization Theory and applications* 106(2), 337–356.

Hodrick, R. J. and E. C. Prescott (1997). Postwar u.s. business cycles: An empirical investigation. *Journal of Money, Credit and Banking* 29(1), 1–16.

Hörmann, S., L. Horváth, and R. Reeder (2013). A functional version of the arch model. *Econometric Theory*, 267–288.

Hörmann, S., L. Kidziński, and M. Hallin (2015). Dynamic functional principal components. *Journal of the Royal Statistical Society: Series B: Statistical Methodology*, 319–348.

Horváth, L. and P. Kokoszka (2012). *Inference for functional data with applications*, Volume 200. Springer Science & Business Media.

Hyndman, R. J. and H. L. Shang (2009). Forecasting functional time series. *Journal of the Korean Statistical Society* 38, 199–211.

Hyndman, R. J. and M. S. Ullah (2007). Robust forecasting of mortality and fertility rates: a functional data approach. *Computational Statistics & Data Analysis* 51(10), 4942–4956.

Kim, S.-J., K. Koh, S. Boyd, and D. Gorinevsky (2009). ℓ_1 trend filtering. *SIAM review* 51(2), 339–360.

Klepsch, J. and C. Klüppelberg (2017). An innovations algorithm for the prediction of functional linear processes. *Journal of Multivariate Analysis* 155, 252–271.

Klepsch, J., C. Klüppelberg, and T. Wei (2017). Prediction of functional arma processes with an application to traffic data. *Econometrics and Statistics* 1, 128–149.

Kokoszka, P. and M. Reimherr (2017). *Introduction to functional data analysis*. CRC press.

Kühnert, S. (2020). Functional arch and garch models: A yule-walker approach. *Electronic Journal of Statistics* 14(2), 4321–4360.

Lounici, K., M. Pontil, S. Van De Geer, A. B. Tsybakov, et al. (2011). Oracle inequalities and optimal inference under group sparsity. *Annals of statistics* 39(4), 2164–2204.

McLennan, W. (1998). Australian social trends 1998. <https://www.abs.gov.au/AUSSTATS/abs@.nsf/DetailsPage/4102.01998?OpenDocument#Publications>.

Menafoglio, A., O. Grujic, and J. Caers (2016). Universal kriging of functional data: Trace-variography vs cross-variography? application to gas forecasting in unconventional shales. *Spatial Statistics* 15, 39–55.

Menafoglio, A., P. Secchi, M. Dalla Rosa, et al. (2013). A universal kriging predictor for spatially dependent functional data of a hilbert space. *Electronic Journal of Statistics* 7, 2209–2240.

Nerini, D., P. Monestiez, and C. Manté (2010). Cokriging for spatial functional data. *Journal of Multivariate Analysis* 101(2), 409–418.

Panaretos, V. M. and S. Tavakoli (2013). Cramér–karhunen–loève representation and harmonic principal component analysis of functional time series. *Stochastic Processes and their Applications* 123(7), 2779–2807.

Ramdas, A. and R. J. Tibshirani (2016). Fast and flexible admm algorithms for trend filtering. *Journal of Computational and Graphical Statistics* 25(3), 839–858.

Ramsay, J. O. (2004). Functional data analysis. *Encyclopedia of Statistical Sciences* 4.

Smola, A. J. and R. Kondor (2003). Kernels and regularization on graphs. In *Learning theory and kernel machines*, pp. 144–158. Springer.

Spangenberg, F. (2013). Strictly stationary solutions of arma equations in banach spaces. *Journal of Multivariate Analysis* 121, 127–138.

Tang, C., T. Wang, and P. Zhang (2020). Functional data analysis: An application to covid-19 data in the united states. *arXiv preprint arXiv:2009.08363*.

Tibshirani, R. (1996). Regression shrinkage and selection via the lasso. *Journal of the Royal Statistical Society: Series B (Methodological)* 58(1), 267–288.

Tibshirani, R., M. Saunders, S. Rosset, J. Zhu, and K. Knight (2005). Sparsity and smoothness via the fused lasso. *Journal of the Royal Statistical Society: Series B (Statistical Methodology)* 67(1), 91–108.

Tibshirani, R. J. et al. (2014). Adaptive piecewise polynomial estimation via trend filtering. *The Annals of Statistics* 42(1), 285–323.

van Delft, A., M. Eichler, et al. (2018). Locally stationary functional time series. *Electronic Journal of Statistics* 12(1), 107–170.

Wang, Y.-X., J. Sharpnack, A. J. Smola, and R. J. Tibshirani (2016). Trend filtering on graphs. *The Journal of Machine Learning Research* 17(1), 3651–3691.

Yuan, M. and Y. Lin (2006). Model selection and estimation in regression with grouped variables. *Journal of the Royal Statistical Society: Series B (Statistical Methodology)* 68(1), 49–67.